Measurement of Forward-Backward Asymmetry and Wilson Coefficients in $B \to K^* l^+ l^-$

A. Ishikawa,[43] K. Abe,[6] I. Adachi,[6] H. Aihara,[43] D. Anipko,[1] Y. Asano,[47] T. Aushev,[10] A. M. Bakich,[38] V. Balagura,[10] M. Barbero,[5] U. Bitenc,[11] I. Bizjak,[11] S. Blyth,[20] A. Bondar,[1] A. Bozek,[23] M. Bračko,[6,16,11] T. E. Browder,[5] P. Chang,[22] Y. Chao,[22] A. Chen,[20] B. G. Cheon,[3] Y. Choi,[37] Y. K. Choi,[37] A. Chuvikov,[31] J. Dalseno,[17] M. Danilov,[10] M. Dash,[48] A. Drutskoy,[4] S. Eidelman,[1] S. Fratina,[11] N. Gabyshev,[1] T. Gershon,[6] G. Gokhroo,[39] B. Golob,[15,11] A. Gorišek,[11] H. Ha,[13] J. Haba,[6] T. Hara,[28] K. Hayasaka,[18] H. Hayashii,[19] M. Hazumi,[6] L. Hinz,[14] T. Hokuue,[18] Y. Hoshi,[41] S. Hou,[20] W.-S. Hou,[22] Y. B. Hsiung,[22] T. Iijima,[18] K. Ikado,[18] K. Inami,[18] H. Ishino,[44] R. Itoh,[6] M. Iwasaki,[43] Y. Iwasaki,[6] J. H. Kang,[49] S. U. Kataoka,[19] N. Katayama,[6] H. Kawai,[2] T. Kawasaki,[25] H. R. Khan,[44] H. Kichimi,[6] S. K. Kim,[35] S. M. Kim,[37] K. Kinoshita,[4] S. Korpar,[16,11] P. Križan,[15,11] R. Kulasiri,[4] R. Kumar,[29] C. C. Kuo,[20] Y.-J. Kwon,[49] J. Lee,[35] S. E. Lee,[35] T. Lesiak,[23] J. Li,[34] A. Limosani,[6] S.-W. Lin,[22] D. Liventsev,[10] G. Majumder,[39] F. Mandl,[8] T. Matsumoto,[45] A. Matyja,[23] S. McOnie,[38] W. Mitaroff,[8] K. Miyabayashi,[19] H. Miyake,[28] H. Miyata,[25] Y. Miyazaki,[18] R. Mizuk,[10] G. R. Moloney,[17] T. Nagamine,[42] E. Nakano,[27] M. Nakao,[6] Z. Natkaniec,[23] S. Nishida,[6] O. Nitoh,[46] T. Nozaki,[6] T. Ohshima,[18] T. Okabe,[18] S. Okuno,[12] S. L. Olsen,[5] Y. Onuki,[25] H. Ozaki,[6] C. W. Park,[37] R. Pestotnik,[11] L. E. Piilonen,[48] M. Rozanska,[23] Y. Sakai,[6] N. Sato,[18] N. Satoyama,[36] T. Schietinger,[14] O. Schneider,[14] C. Schwanda,[8] A. J. Schwartz,[4] R. Seidl,[32] K. Senyo,[18] M. E. Sevior,[17] M. Shapkin,[9] H. Shibuya,[40] A. Somov,[4] N. Soni,[29] R. Stamen,[6] S. Stanič,[26] M. Starič,[11] H. Stoeck,[38] K. Sumisawa,[28] S. Suzuki,[33] O. Tajima,[6] F. Takasaki,[6] K. Tamai,[6] N. Tamura,[25] M. Tanaka,[6] G. N. Taylor,[17] Y. Teramoto,[27] X. C. Tian,[30] K. Trabelsi,[5] T. Tsukamoto,[6] S. Uehara,[6] S. Uno,[6] P. Urquijo,[17] Y. Ushiroda,[6] Y. Usov,[1] G. Varner,[5] S. Villa,[14] C. C. Wang,[22] C. H. Wang,[21] M.-Z. Wang,[22] Y. Watanabe,[44] E. Won,[13] Q. L. Xie,[7] B. D. Yabsley,[38] A. Yamaguchi,[42] Y. Yamashita,[24] M. Yamauchi,[6] J. Ying,[30] Y. Yusa,[48] J. Zhang,[6] L. M. Zhang,[34] and Z. P. Zhang[34]

(Belle Collaboration)

[1]*Budker Institute of Nuclear Physics, Novosibirsk*
[2]*Chiba University, Chiba*
[3]*Chonnam National University, Kwangju*
[4]*University of Cincinnati, Cincinnati, Ohio 45221*
[5]*University of Hawaii, Honolulu, Hawaii 96822*
[6]*High Energy Accelerator Research Organization (KEK), Tsukuba*
[7]*Institute of High Energy Physics, Chinese Academy of Sciences, Beijing*
[8]*Institute of High Energy Physics, Vienna*
[9]*Institute of High Energy Physics, Protvino*
[10]*Institute for Theoretical and Experimental Physics, Moscow*
[11]*J. Stefan Institute, Ljubljana*
[12]*Kanagawa University, Yokohama*
[13]*Korea University, Seoul*
[14]*Swiss Federal Institute of Technology of Lausanne, EPFL, Lausanne*
[15]*University of Ljubljana, Ljubljana*
[16]*University of Maribor, Maribor*
[17]*University of Melbourne, Victoria*
[18]*Nagoya University, Nagoya*
[19]*Nara Women's University, Nara*
[20]*National Central University, Chung-li*
[21]*National United University, Miao Li*
[22]*Department of Physics, National Taiwan University, Taipei*
[23]*H. Niewodniczanski Institute of Nuclear Physics, Krakow*
[24]*Nippon Dental University, Niigata*
[25]*Niigata University, Niigata*
[26]*Nova Gorica Polytechnic, Nova Gorica*
[27]*Osaka City University, Osaka*
[28]*Osaka University, Osaka*
[29]*Panjab University, Chandigarh*
[30]*Peking University, Beijing*
[31]*Princeton University, Princeton, New Jersey 08544*

0031-9007/06/96(25)/251801(6)

[32]*RIKEN BNL Research Center, Upton, New York 11973*
[33]*Saga University, Saga*
[34]*University of Science and Technology of China, Hefei*
[35]*Seoul National University, Seoul*
[36]*Shinshu University, Nagano*
[37]*Sungkyunkwan University, Suwon*
[38]*University of Sydney, Sydney NSW*
[39]*Tata Institute of Fundamental Research, Bombay*
[40]*Toho University, Funabashi*
[41]*Tohoku Gakuin University, Tagajo*
[42]*Tohoku University, Sendai*
[43]*Department of Physics, University of Tokyo, Tokyo*
[44]*Tokyo Institute of Technology, Tokyo*
[45]*Tokyo Metropolitan University, Tokyo*
[46]*Tokyo University of Agriculture and Technology, Tokyo*
[47]*University of Tsukuba, Tsukuba*
[48]*Virginia Polytechnic Institute and State University, Blacksburg, Virginia 24061*
[49]*Yonsei University, Seoul*
(Received 8 March 2006; published 26 June 2006)

We report the first measurement of the forward-backward asymmetry and the ratios of Wilson coefficients A_9/A_7 and A_{10}/A_7 in $B \to K^* \ell^+ \ell^-$, where ℓ represents an electron or a muon. We find evidence for the forward-backward asymmetry with a significance of 3.4σ. The results are obtained from a data sample containing 386×10^6 $B\bar{B}$ pairs that were collected on the $\Upsilon(4S)$ resonance with the Belle detector at the KEKB asymmetric-energy e^+e^- collider.

DOI: 10.1103/PhysRevLett.96.251801 PACS numbers: 12.15.Ji, 11.30.Er, 11.30.Hv, 13.20.He

Flavor-changing neutral current $b \to s$ processes proceed via loop diagrams in the standard model (SM). If additional diagrams with non-SM particles contribute to such processes, the decay rate and kinematics are modified. Such contributions may change the 12 Wilson coefficients [1] that parametrize the strength of the weak and strong short distance interactions. The $b \to s\ell^+\ell^-$ amplitude is described by the effective Wilson coefficients C_7, C_9, and C_{10}, whose terms have been calculated up to next-to-next-to-leading order (NNLO) [2] in quantum chromodynamics. To evaluate the Wilson coefficients, we use A_i which are dominant and q^2-independent real terms of C_i. Other small complex terms in C_i are fixed to the SM values. Here, q^2 is the squared invariant mass of the dilepton system.

The magnitude of A_7 is strongly constrained from measurements of $B \to X_s\gamma$ [3,4], where X_s is a hadronic system with an s quark; a large area of the (A_9, A_{10}) plane is excluded by branching fraction measurements of $B \to X_s\ell^+\ell^-$ and $B \to K^{(*)}\ell^+\ell^-$ [5–8], where $K^{(*)}$ refers to K or K^*. However, the sign of A_7 and the values of A_9 and A_{10} are not yet determined. Measurement of the forward-backward asymmetry and differential decay rate as functions of q^2 and θ for $B \to K^*\ell^+\ell^-$ constrains the relative signs and magnitudes of these coefficients [9,10]. Here θ is the angle between the momenta of the negative (positive) lepton and the B ($\bar{B}$) meson in the dilepton rest frame. The forward-backward asymmetry is defined using the differential decay width $g(q^2, \theta) = d^2\Gamma/dq^2 d\cos\theta$ [11] as

$$\mathcal{A}_{\rm FB}(q^2) = \frac{\int_{-1}^{1} \mathrm{sgn}(\cos\theta) g(q^2, \theta) d\cos\theta}{\int_{-1}^{1} g(q^2, \theta) d\cos\theta}. \qquad (1)$$

The numerator in Eq. (1) can be expressed in terms of Wilson coefficients as

$$\int_{-1}^{1} \mathrm{sgn}(\cos\theta) g(q^2, \theta) d\cos\theta = -C_{10}\xi(q^2) \times \left(\mathrm{Re}(C_9)F_1 + \frac{1}{q^2}C_7F_2\right), \qquad (2)$$

where ξ is a function of q^2, while F_1 and F_2 depend on form factors. (The full expression can be found in Ref. [11].)

In this Letter, we report the first measurement of the forward-backward asymmetry and ratios of Wilson coefficients in $B \to K^*\ell^+\ell^-$. We use a 357 fb^{-1} data sample containing 386×10^6 $B\bar{B}$ pairs taken at the $\Upsilon(4S)$ resonance. We also study the $B^+ \to K^+\ell^+\ell^-$ mode, which is expected to have a very small forward-backward asymmetry even in the presence of new physics [12]. Charge-conjugate modes are included throughout this Letter.

The data were taken at the KEKB collider [13] and collected with the Belle detector [14]. The detector consists of a silicon vertex detector, a central drift chamber, aerogel Cherenkov counters, time-of-flight scintillation counters, an electromagnetic calorimeter, and a muon identification system.

The event reconstruction procedure is the same as described in our previous Letter [5]. The following final states are used to reconstruct B candidates: $K^{*0}\ell^+\ell^-$, $K^{*+}\ell^+\ell^-$, and $K^+\ell^+\ell^-$, with subdecays $K^{*0} \to K^+\pi^-$, $K^{*+} \to K_S^0\pi^+$ and $K^+\pi^0$, $K_S^0 \to \pi^+\pi^-$, and $\pi^0 \to \gamma\gamma$.

Hereafter, $K^{*0}\ell^+\ell^-$ and $K^{*+}\ell^+\ell^-$ are combined and called $K^*\ell^+\ell^-$.

We use two variables defined in the center-of-mass (c.m.) frame to select B candidates: the beam-energy constrained mass $M_{\rm bc} = \sqrt{(E^*_{\rm beam}/c^2)^2 - (p^*_B/c)^2}$ and the energy difference $\Delta E = E^*_B - E^*_{\rm beam}$, where p^*_B and E^*_B are the measured c.m. momentum and energy of the B candidate, and $E^*_{\rm beam}$ is the c.m. beam energy. When multiple candidates are found in an event, we select the candidate with the smallest value of $|\Delta E|$.

The dominant background consists of $B\bar{B}$ events where both B mesons decay semileptonically. We suppress this background using missing energy and $\cos\theta^*_B$, where θ^*_B is the angle between the flight direction of the B meson and the beam axis in the c.m. frame. These quantities are combined to form signal and background likelihoods $\mathcal{L}_{\rm sig}$ and $\mathcal{L}_{B\bar{B}}$, respectively, and event selection is then performed using the ratio $\mathcal{R}_{B\bar{B}} = \mathcal{L}_{\rm sig}/(\mathcal{L}_{\rm sig} + \mathcal{L}_{B\bar{B}})$. The continuum ($e^+e^- \to q\bar{q}$, $q = u, d, s, c$) background is suppressed using a likelihood ratio $\mathcal{R}_{\rm cont}$ (defined similarly to $\mathcal{R}_{B\bar{B}}$) that depends on three variables: a Fisher discriminant [15] calculated from the sum of c.m. energies of the final state particles in each of nine cones along the B candidate c.m. sphericity axis [16] and the normalized second Fox-Wolfram moment [17], the angle between the beam axis and the c.m. sphericity axis, and $\cos\theta^*_B$. Backgrounds from $B \to J/\psi X_s$ and $B \to \psi(2S)X_s$ decays, referred to below as $B \to \psi X_s$, are rejected using the dilepton invariant mass. Backgrounds from photon conversions and π^0 Dalitz decays are suppressed by requiring the e^+e^- invariant mass to be above 140 MeV$/c^2$.

The signal box is defined as $|M_{\rm bc} - m_B| < 8$ MeV$/c^2$ for both lepton modes and $-55(-35)$ MeV $< \Delta E <$ 35 MeV for the electron (muon) mode. We optimize the selections on $\mathcal{R}_{\rm cont}$ and $\mathcal{R}_{B\bar{B}}$ for each K^* decay mode and each lepton mode to maximize sensitivity to events with $q^2 < 6$ GeV$^2/c^2$ assuming the branching fractions in Ref. [18].

To determine the signal yield, we perform an unbinned maximum-likelihood fit to the $M_{\rm bc}$ distribution for events that lie within the ΔE signal window. The fit function includes signal, cross feeds, and other background components. The cross feeds are misreconstructed $K^{(*)}\ell^+\ell^-$ events with correct ("CF") and incorrect ("IF") B meson flavor assignment. The cross feed from $X_s\ell^+\ell^-$ events other than $K^{(*)}\ell^+\ell^-$ is negligible. The other backgrounds come from dilepton background, combinatorial $K^{(*)}\ell^\pm h^\mp$, $K^{(*)}h^+h^-$, and ψX_s events, where h represents a pion or a kaon. The dilepton background refers to the sum of all background sources with two leptons where the lepton is from leptonic or semileptonic meson decays, photon conversions, and π^0 Dalitz decays. The $K^{(*)}h^+h^-$ background is from both combinatorial background and B meson decays.

The shape for cross-feed events is parametrized by a sum of an ARGUS function [19] and a Gaussian whose parameters are determined from Monte Carlo (MC) samples. The dilepton background is modeled by an ARGUS function. The shape of each background is determined from a MC sample. (The $K^{(*)}e^\pm\mu^\mp$ background shape is found to be consistent between the MC sample and data.) Since the shape for $K^{(*)}\ell^\pm h^\mp$ is similar to that for the dilepton background, we use the same parametrizations for both backgrounds. The residual background from ψX_s is estimated from a MC sample of ψ inclusive events and parametrized by the sum of an ARGUS function and a Gaussian. The background from events with misidentified leptons is also parametrized by the sum of an ARGUS function and a Gaussian. In the fit, all background fractions except the dilepton background are fixed while the signal fraction is allowed to float.

Figure 1 shows the fit result. We obtain 113.6 ± 13.0 and 96.0 ± 12.0 signal events for $K^*\ell^+\ell^-$ and $K^+\ell^+\ell^-$, respectively.

We use $B \to K^*\ell^+\ell^-$ candidates in the signal box to measure the normalized double differential decay width. For the evaluation of the Wilson coefficients, the full (partial) NNLO Wilson coefficients C_i [2,7] are used for $q^2/m_b^2 < 0.25$ (> 0.25). The value of A_7 is fixed at the SM value -0.330 or the sign-flipped value $+0.330$. The SM values for A_9 and A_{10} are 4.07 and -4.21, respectively [7]. We choose A_9/A_7 and A_{10}/A_7 as fit parameters. To extract these ratios, we perform an unbinned maximum-likelihood fit to the events in the signal box with a probability density function (PDF) that includes the normalized double differential decay width. The PDF used for the fit consists of terms describing the signal, cross feeds, and backgrounds:

$$\begin{aligned} P(M_{\rm bc}, q^2, \cos\theta; A_9/A_7, A_{10}/A_7) = {} & \frac{1}{N_{\rm sig}} f_{\rm sig}\epsilon_{\rm sig}(q^2, \cos\theta) g(q^2, \cos\theta) + \frac{1}{N_{\rm CF}} f_{\rm CF}\epsilon_{\rm CF}(q^2, \cos\theta) g(q^2, \cos\theta) \\ & + \frac{1}{N_{\rm IF}} f_{\rm IF}\epsilon_{\rm IF}(q^2, \cos\theta) g(q^2, -\cos\theta) + (1 - f_{\rm sig} - f_{\rm CF} - f_{\rm IF} - f_{K^*hh} - f_{\psi X_s}) \\ & \times \{(f_{K^*\ell h}\mathcal{P}_{K^*\ell h}(q^2, \cos\theta) + (1 - f_{K^*\ell h})\mathcal{P}_{\rm dl}(q^2, \cos\theta)\} + f_{K^*hh}\mathcal{P}_{K^*hh}(q^2, \cos\theta) \\ & + f_{\psi X_s}\mathcal{P}_{\psi X_s}(q^2, \cos\theta). \end{aligned} \tag{3}$$

Here $\mathcal{P}_{K^*\ell h}$, $\mathcal{P}_{\rm dl}$, $\mathcal{P}_{K^*hh}$, and $\mathcal{P}_{\psi X_s}$ are the probability density functions for $K^*\ell h$, dilepton background, K^*hh, and ψX_s, respectively. The quantities $\epsilon_{\rm sig}$ ($N_{\rm sig}$), $\epsilon_{\rm CF}$ ($N_{\rm CF}$), and $\epsilon_{\rm IF}$ ($N_{\rm IF}$) correspond to the efficiency function (normalization) of

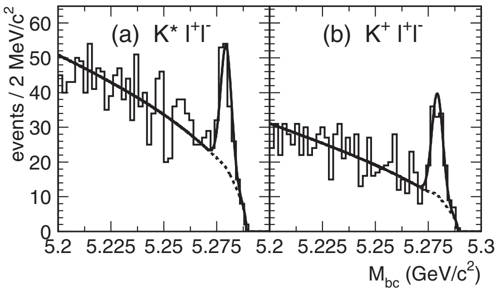

FIG. 1. $M_{\rm bc}$ distributions for (a) $B \to K^* \ell^+ \ell^-$ and (b) $B \to K^+ \ell^+ \ell^-$ samples. The solid and dashed curves are the fit results for the total and background contributions, respectively.

each signal and cross-feed component. Each fraction f is the probability of finding the corresponding component in the data sample for a given $M_{\rm bc}$ value determined from the $M_{\rm bc}$ fit, with the exception of $f_{K^*\ell h}$, which is the fraction of the $K^*\ell h$ events within the background component with misidentification leptons determined from the MC samples. The functions ϵ and $\mathcal{P}$ for the dilepton background, $K^*\ell^\pm h^\mp$, and ψX_s are obtained from MC samples. The $K^* h^+ h^-$ background shape $\mathcal{P}_{K^*hh}$ is obtained from $K^* h^+ h^-$ events and the momentum- and angular-dependent hadron to lepton misidentification probability.

The renormalization scale μ is set to 2.5 GeV as suggested by Ref. [7]. The double differential decay width includes the form factor parameters and the bottom quark mass m_b. We choose the form factor model of Refs. [7,11] and a bottom quark mass of 4.8 GeV/c^2.

First, we measure the asymmetry $\tilde{\mathcal{A}}_{\rm FB}$, which is defined as

$$\tilde{\mathcal{A}}_{\rm FB} = \frac{\iint_{-1}^{1} \mathrm{sgn}(\cos\theta) g(q^2, \theta) d\cos\theta dq^2}{\iint_{-1}^{1} g(q^2, \theta) d\cos\theta dq^2}. \quad (4)$$

We determine the yield in five q^2 bins for $\cos\theta > 0$ and $\cos\theta < 0$ from a fit to the $M_{\rm bc}$ distribution. After efficiency correction for each bin, we obtain

$$\begin{aligned} \tilde{\mathcal{A}}_{\rm FB}(B \to K^* \ell^+ \ell^-) &= 0.50 \pm 0.15 \pm 0.02, \\ \tilde{\mathcal{A}}_{\rm FB}(B^+ \to K^+ \ell^+ \ell^-) &= 0.10 \pm 0.14 \pm 0.01, \end{aligned} \quad (5)$$

where the first error is statistical and the second is systematic. A large asymmetry is measured for $K^* \ell^+ \ell^-$ with a significance of 3.4σ. The result for $K^+ \ell^+ \ell^-$ is consistent with zero as expected.

We fit the $K^* \ell^+ \ell^-$ candidates with the PDF of Eq. (3). The fit results of ratios of Wilson coefficients are summarized in Table I. Figure 2 shows the fit results projected onto the background-subtracted forward-backward asymmetry distribution in bins of q^2.

We estimate contributions to the systematic error due to uncertainties in the physics parameters, finite q^2 resolution, efficiency, and signal probability. We vary the A_7 value within the range allowed by the branching fraction of $B \to X_s \gamma$ [20]. The bottom quark mass m_b is varied by $\pm 0.2\ \mathrm{GeV}/c^2$. The systematic uncertainty associated with the choice of the form factor model is taken from the deviation in fit results when a model of Ref. [21] is used. The effect of q^2 resolution is estimated using a toy MC study. The effect due to $\cos\theta$ resolution is found to be negligible. The uncertainty in the efficiency is estimated by changing the efficiency for pions with $p < 0.3\ \mathrm{GeV}/c$, electrons with $p < 0.7\ \mathrm{GeV}/c$, and muons with $p < 1\ \mathrm{GeV}/c$ by 10%, 5%, and 10%, respectively, to obtain revised efficiency functions for signal and background PDFs. We change the shape parameters for the signal or background probability functions f and take the difference as an uncertainty in the signal fraction. The parameters are modified by $\pm 1\sigma$ for signal, dilepton background, and $K^* h^+ h^-$. We vary the normalization for cross-feed events and ψX_s by 100% since we cannot determine these background from data. To assign the systematic error due to the uncertainty in the fraction of $K^* \ell^\pm h^\mp$, we change the value of $f_{K^*\ell h}$ by 20%, which corresponds to the difference between the MC sample and sideband events. Table II summarizes the contributions to the systematic error.

The fit results are consistent with the SM values $A_9/A_7 = -12.3$ and $A_{10}/A_7 = 12.8$. In Fig. 3, we show

TABLE I. A_9/A_7 and A_{10}/A_7 fit results for negative and positive A_7 values. The first error is statistical and the second is systematic.

	$A_7 = -0.330$	$A_7 = +0.330$
A_9/A_7	$-15.3^{+3.4}_{-4.8} \pm 1.1$	$-16.3^{+3.7}_{-5.7} \pm 1.4$
A_{10}/A_7	$10.3^{+5.2}_{-3.5} \pm 1.8$	$11.1^{+6.0}_{-3.9} \pm 2.4$

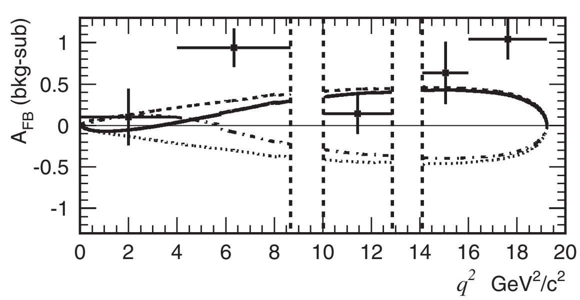

FIG. 2. Fit result for the negative A_7 solution (solid line) projected onto the background-subtracted forward-backward asymmetry and forward-backward asymmetry curves for several input parameters, including the effects of efficiency: A_7 positive case ($A_7 = 0.330$, $A_9 = 4.07$, $A_{10} = -4.21$) (dashed line), A_{10} positive case ($A_7 = -0.280$, $A_9 = 2.42$, $A_{10} = 1.32$) (dotted-dashed line), and both A_7 and A_{10} positive cases ($A_7 = 0.280$, $A_9 = 2.22$, $A_{10} = 3.82$) (dotted line) [9]. The new physics scenarios shown by the dotted-dashed and dotted curves are excluded. The blank regions are excluded by the ψX_s veto.

TABLE II. Summary of systematic errors.

	$A_7 = -0.330$		$A_7 = +0.330$	
Source	A_9/A_7	A_{10}/A_7	A_9/A_7	A_{10}/A_7
A_7 [20]	$+0.2 - 0.0$	±0.0	$+0.1 - 0.2$	$+0.3 - 0.1$
m_b (4.8 ± 0.2 GeV$/c^2$)	±0.7	±0.5	±0.6	±0.4
Model dependence	±0.7	±1.7	±1.0	±2.2
q^2 resolution	±0.3	±0.4	±0.3	±0.4
Efficiency	±0.1	±0.0	±0.1	±0.1
Signal probability	$+0.4 - 0.5$	$+0.2 - 0.3$	$+0.4 - 0.5$	±0.4
Total	±1.1	±1.8	$+1.3 - 1.4$	$+2.4 - 2.3$

confidence level (C.L.) contours in the $(A_9/A_7, A_{10}/A_7)$ plane based on the fit likelihood smeared by the systematic error, which is assumed to have a Gaussian distribution. We also calculate an interval in A_9A_{10}/A_7^2 at the 95% C.L. for the allowed A_7 region,

$$-14.0 \times 10^2 < A_9A_{10}/A_7^2 < -26.4. \tag{6}$$

From this, the sign of A_9A_{10} must be negative, and the solutions in quadrants I and III in Fig. 3 are excluded at the 98.2% confidence level. Since solutions in both quadrants II and IV are allowed, we cannot determine the sign of A_7A_{10}. Figure 2 shows the comparison between the fit results for the negative A_7 value projected onto the forward-backward asymmetry and the forward-backward asymmetry distributions for several input parameters. We exclude the new physics scenarios shown by the dotted and dotted-dashed curves, which have a positive A_9A_{10} value.

In summary, we have measured the ratios of Wilson coefficients in $B \to K^*\ell^+\ell^-$ decay for the first time by studying the forward-backward asymmetry in the angular distribution of leptons. We find evidence for a large forward-backward asymmetry with a significance of 3.4σ. The fit results are consistent with the SM prediction and also with the case where the sign of A_7A_{10} is flipped. We exclude new physics scenarios with positive A_9A_{10} at 98.2% confidence.

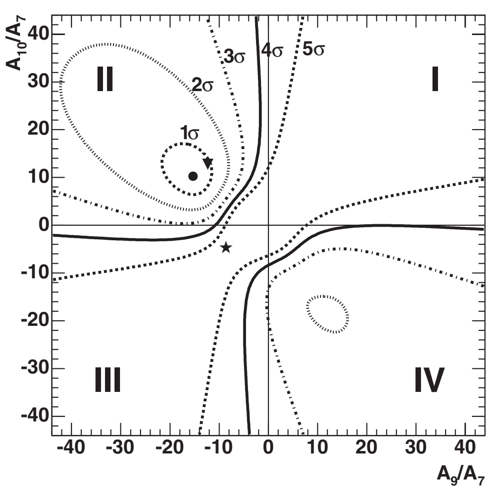

FIG. 3. C.L. contours for negative A_7. Curves show 1σ–5σ contours. The symbols show the fit (circle), SM (triangle), and A_{10}-positive (star) [9] cases. The A_{10}-positive case appears as the dotted-dashed curve of Fig. 2.

We thank Gudrun Hiller and Enrico Lunghi for their invaluable suggestions. We thank the KEKB group for excellent operation of the accelerator, the KEK cryogenics group for efficient solenoid operations, and the KEK computer group and the NII for valuable computing and Super-SINET network support. We acknowledge support from MEXT and JSPS (Japan); ARC and DEST (Australia); NSFC and KIP of CAS (contract No. 10575109 and IHEP-U-503, China); DST (India); the PBRG of KRF, and the CHEP SRC and BR (grant No. R01-2005-000-10089-0) programs of KOSEF (Korea); KBN (contract No. 2P03B 01324, Poland); MIST (Russia); ARRS (Slovenia); SNSF (Switzerland); NSC and MOE (Taiwan); and DOE (USA).

[1] See, for example, G. Buchalla *et al.*, Rev. Mod. Phys. **68**, 1125 (1996).

[2] H. H. Asatryan *et al.*, Phys. Lett. B **507**, 162 (2001).

[3] B. Aubert *et al.* (*BABAR* Collaboration), Phys. Rev. D **72**, 052004 (2005); P. Koppenburg *et al.* (Belle Collaboration), Phys. Rev. Lett. **93**, 061803 (2004); S. Chen *et al.* (CLEO Collaboration), Phys. Rev. Lett. **87**, 251807 (2001); R. Barate *et al.* (ALEPH Collaboration), Phys. Lett. B **429**, 169 (1998).

[4] T. Besmer *et al.*, Nucl. Phys. **B609**, 359 (2001); C. Bobeth *et al.*, Nucl. Phys. **B567**, 153 (2000); F. Borzumati *et al.*, Phys. Rev. D **62**, 075005 (2000); M. Ciuchini *et al.*, Nucl. Phys. **B534**, 3 (1998); T. Goto *et al.*, Phys. Rev. D **58**, 094006 (1998).

[5] A. Ishikawa *et al.* (Belle Collaboration), Phys. Rev. Lett. **91**, 261601 (2003).

[6] M. Iwasaki *et al.* (Belle Collaboration), Phys. Rev. D **72**, 092005 (2005); B. Aubert *et al.* (*BABAR* Collaboration), Phys. Rev. Lett. **93**, 081802 (2004); **91**, 221802 (2003).

[7] A. Ali *et al.*, Phys. Rev. D **66**, 034002 (2002).

[8] P. Gambino *et al.*, Phys. Rev. Lett. **94**, 061803 (2005).

[9] E. Lunghi *et al.*, Nucl. Phys. **B568**, 120 (2000).

[10] J. L. Hewett and J. D. Wells, Phys. Rev. D **55**, 5549 (1997); A. Ali *et al.*, Z. Phys. C **67**, 417 (1995); N. G. Deshpande

et al., Phys. Lett. B **308**, 322 (1993); B. Grinstein *et al.*, Nucl. Phys. **B319**, 271 (1989); W. S. Hou *et al.*, Phys. Rev. Lett. **58**, 1608 (1987).
[11] A. Ali *et al.*, Phys. Rev. D **61**, 074024 (2000).
[12] D. A. Demir *et al.*, Phys. Rev. D **66**, 034015 (2002).
[13] S. Kurokawa and E. Kikutani, Nucl. Instrum. Methods Phys. Res., Sect. A **499**, 1 (2003), and other papers included in this volume.
[14] A. Abashian *et al.* (Belle Collaboration), Nucl. Instrum. Methods Phys. Res., Sect. A **479**, 117 (2002); Y. Ushiroda (Belle SVD2 Group), Nucl. Instrum. Methods Phys. Res., Sect. A **511**, 6 (2003).
[15] R. A. Fisher, Ann. Eugen. **7**, 179 (1936).
[16] For example, V. Barger and R. Phillips, *Collider Physics* (Addison-Wesley, Reading, MA, 1987).
[17] G. C. Fox and S. Wolfram, Phys. Rev. Lett. **41**, 1581 (1978).
[18] Heavy Flavor Averaging Group (HFAG), hep-ex/0505100.
[19] H. Albrecht *et al.* (ARGUS Collaboration), Phys. Lett. B **241**, 278 (1990).
[20] G. Hiller (private communication). Hiller calculates an A_7 interval based on HFAG winter 2005 results [18], $0.25 < A_7 < 0.41$ and $-0.35 < A_7 < -0.21$ at 68% C.L. for the positive and negative solutions, respectively.
[21] D. Melikhov *et al.*, Phys. Lett. B **410**, 290 (1997).